Proceedings of the ASME 2010 3rd Joint US-European Fluids Engineering Summer Meeting and 8th International Conference on Nanochannels, Microchannels, and Minichannels
FEDSM-ICNMM2010
August 1-5, 2010, Montreal, Canada

FEDSM-ICNMM2010-30451

MICROFLUIDIC CONCENTRATION OF SAMPLE SOLUTES USING JOULE HEATING EFFECTS UNDER COMBINED AC AND DC ELECTRIC FIELD

Zhengwei Ge, Chun Yang

School of Mechanical and Aerospace Engineering, Nanyang Technological University,
50 Nanyang Avenue, Singapore 639798

ABSTRACT

Microfluidic concentration is achieved by utilizing Joule heating effect induced temperature gradient focusing (TGF) under a combined AC and DC electric field imposed in a straight microchannel with sudden expansion in cross-section. The introduction of AC electric field component services dual functions: one is to produce Joule heating effects for generating temperature gradient, and the other is to suppress electroosmotic flow with high frequencies. Therefore, the required DC voltage for achieving sample concentration with Joule heating induced TGF technique is remarkably reduced. The lower DC voltage can lead to smaller electroosmotic flow (EOF), thereby reducing the backpressure effect due to the finite reservoir size. It was demonstrated that using the proposed new TGF technique with Joule heating effect under a combined AC and DC field, more than 2500-fold concentration enhancement was obtained within 14 minutes in a PDMS/PDMS microdevice, which is an order of magnitude higher than the literature reported concentration enhancement achieved by microfluidic devices utilizing the Joule heating induced TGF technique.

KEYWORDS: Joule heating, temperature gradient focusing, sample concentration, combined AC and DC electric field

NOMENCLATURE

C	concentration of the sample solutes [M]
c_p	specific heat capacity [$Jkg^{-1}K^{-1}$]
D	mass diffusion coefficient of the solutes [m^2s^{-1}]
$\vec{E}$	strength of the applied electric field [Vm^{-1}]
Jo	Joule number, $L^2\lambda\vec{E}\cdot\vec{E}/\left[k(T_0-T_{ref})\right]$
k	thermal conductivity [$Wm^{-1}K^{-1}$]
p	hydrodynamic pressure [Nm^{-2}]
Pr	Prandtl number
Re	Reynolds number
Sc	Schmit number
t	time [s]
T	temperature [K]
u	bulk fluid velocity [ms^{-1}]
U_s	Smoluchowski velocity [ms^{-1}]
u_{ep}	electrophoretic velocity [ms^{-1}]
V	voltage [V]

Greek symbols

μ_{EP}	electrophoretic mobility [$m^2V^{-1}s^{-1}$]
ε_0	dielectric constant of vacuum [Fm^{-1}]
ε_m	dielectric constant of electrolyte solution [Fm^{-1}]
λ	electrical conductivity of electrolyte solution [Sm^{-1}]
ρ	density of electrolyte solution [kgm^{-3}]
ρ_e	net charge density of electrolyte solution [Cm^{-2}]
ϕ	electric potential [V]
η	dynamic viscosity of electrolyte solution [Nsm^{-2}]
ζ_w	zeta potential of the channel wall [V]

Subscribt

ref	reference parameters

1. INTRODUCTION

Nowadays, microfluidics has attracted lots of attentions due to its promising applications in biotechnology, medicine, and chemistry [1-3]. Concentration of samples is a significant challenge in the design and operation of microfluidic chemical or biochemical devices, because the concentration of original samples is often too dilute for adequate detection. Furthermore, in microfluidic channels, the amount of sample volumes handled is very small and the detection length is very short,

which already push the detection technology to its limit [4]. Hence, it will be advantageous to preconcentrate analytes before detection or further manipulation.

Several techniques have been developed for preconcentration of sample analytes. One group of concentration techniques termed as the stacking methods is based on a difference in analytes velocity within two different buffer regions, when the analytes migrate from a faster velocity zone into a slower velocity zone so that analytes are concentrated. The stacking methods include the field amplified sample stacking method [5][6], the sweeping method [7][8] and the isotachophoresis [9][10]. However, in sample stacking process, the concentration enhancement is limited by the magnitude of analyte velocity change ratio [11]. Another group of analyte concentration methods is termed as field gradient focusing methods, including the isoelectric focusing (IEF) [12-14], the electric field gradient focusing (EFGF) [15-17] and the temperature gradient focusing (TGF) [18-25]. For the field gradient focusing methods, analytes are focused at a unique equilibrium point where their net velocity is zero. The concentration enhancement in focusing techniques is determined by the rate at which analytes are transported to the focusing zone and the duration of the application of the focusing field, allowing for high resolution and sensitivity.

TGF is a newly developed field gradient focusing method based on which the concentration of sample analytes is achieved by balancing the electrophoretic motion of analytes against the bulk flow of buffer solution. The technique is demonstrated for a variety of analytes, including fluorescent dyes, amino acids, DNA, proteins, and particles (polystyrene) [18]. The possibly achieved high concentration and required relatively short channels (e.g., 4mm) make TGF well suitable for development of integrated microfluidic systems, with promising in combination with other concentration and separation techniques, such as the micellar affinity gradient focusing (MAGF) [19], the field-amplified continuous sample injection (FACSI) [20] etc. Applications in DNA hybridization [21] and chiral separations [22] have also been demonstrated. Effect of finite sample was presented by Lin et al [23] to address the nonlinear sample-buffer interactions in TGF. Huber and Santiago [24, 25] developed a 1-D model of dispersion in TGF with experimental demonstration.

In TGF, the required temperature gradient can be induced either by external heating/cooling equipment or by inherent Joule heating resulted from applied electric field [26-28]. There are several advantages of using Joule heating to induce the temperature gradient in TGF compared with using external heating/cooling equipment. It consumes less power. The electric field used for generating Joule heat can also be used to drive the flow, which makes the design simple. Importantly, the device is more portable without need of bulky external heating units.

A thorough study of TGF with Joule heating achieved in a microchannel under a sole DC voltage was detailed previously [29]. The effects of applied voltage, buffer concentration and channel width ratio were investigated and summarized by using a dimensionless Joule number. Though the achieved concentration enhancement of 450-fold within 75 s is better than previous Joule heating based TGF, it is still not high enough compared with thousands-fold concentration in some other concentration techniques. This letter reports a novel technique of utilizing a combined AC and DC electric field to produce a temperature gradient through inherent Joule heating and to manipulate the EOF and analyte motion in TGF technique. The advantage of using a combined AC and DC electric field is that the AC electric field with a high frequency allows suppressing the EOF while it contributes to producing a Joule heating induced temperature gradient. Hence, the required high DC voltage can be greatly reduced, which in turn can result in smaller EOF and thus less backpressure effect. Therefore, the concentration enhancement can be significantly improved. The proposed technique utilizing a combined AC and DC field can lead to a concentration factor higher than 2500-fold which is almost an order of magnitude higher than the literature reported concentration factors achieved in microfluidic devices using the Joule heating effect induced TGF technique [18][26][29].

2. THEORY

In this study, a combined AC and DC electric field was applied to a microchannel instead of using a sole DC electric field as usually reported in other studies for concentration of sample solutes through the TGF technique with Joule heating effects. The microchannel with a step change in cross-section is designed to achieve TGF with Joule heating effects, as shown in Fig. 1. The model development should include governing equations for the electric potential profiles, bulk flow field, temperature field and sample concentration distributions. According to our previous study [29], the characteristic time scales of the N-S equation $\tau_V \sim O(10^{-3})$ and the energy equation $\tau_T \sim O(10^{-2})$ are about four orders smaller than that of the mass transport equation $\tau_C \sim O(10^{2})$. When the applied AC electric field has a high frequency of 10 kHz, the time period $\tau_{AC} \sim O(10^{-4})$ is much smaller than τ_C. Therefore, the transient concentration field can be solved after we obtain the steady-state electric field, velocity field and temperature field.

2.1 Applied electric field

The time averaged applied electric potential is governed by the Laplace equation which is written as

$$\nabla \cdot \left[\lambda(T) \nabla \phi \right] = 0 \tag{1}$$

As given by Weast et al. [30], the electrical conductivity $\lambda(T)$ can be expressed as

$$\lambda(T) = \lambda_0 \left[1 + 0.02 \left(T - T_0 \right) \right] \tag{2}$$

where λ_0 is the conductivity of the electrolyte at reference temperature T_0. A combined AC and DC voltage is imposed at the inlet reservoir (on the wide channel side), while the outlet

reservoir (on the wide channel side) is grounded, i.e. $\phi_{x=0}=0$ and $\phi_{x=L}=V_{AC+DC}=V_{AC,\,rms}+V_{DC}$, where $V_{AC,\,rms}$ is the root mean square of AC electric field and V_{DC} is the DC bias. Electric insulation condition is applied at the channel wall.

2.2 Bulk solution electroosmotic flow field

The bulk fluid velocity driven by EOF can be described by the Navier-Stokes equation and the continuity equation which are expressed as

$$\rho\vec{u}\cdot\nabla\vec{u}=-\nabla p+\nabla\cdot\left(\eta(T)\nabla\vec{u}\right) \tag{3}$$

$$\nabla\cdot\vec{u}=0 \tag{4}$$

where $\vec{u}$ is the bulk fluid velocity vector, ρ and p are the solution density and hydrodynamic pressure, respectively, $\eta(T)$ is the solution dynamic viscosity whose dependence on temperature is given as $\eta(T)=1.25\times10^{-6}\exp(1958/T)$ [30].

Slip boundary condition is applied at the channel wall, because the electric double layer (*EDL*) thickness is usually of about 1 nm to 100 nm which is relatively thin compared with the channel dimensions (on the order of 100μm), the variation of fluid velocity within the thin *EDL* can be neglected. This well-known slip velocity approximation assumes the channel wall to move with a velocity determined by Smoluchowski's equation given by

$$\vec{U}_s=-\frac{\varepsilon_m\varepsilon_0\zeta_w\vec{E}}{\eta} \tag{5}$$

where ε_m is the solution dielectric constant, ε_0 is the dielectric constant of vacuum, ζ_w is the zeta potential of the channel wall, and $\vec{E}$ is the strength of local applied electric field. The characteristic response time of an electroosmotic flow after switching on the electric field can be estimated from $\tau_{eof}=O\left(D_h^2\rho/\eta\right)$, where D_h is the hydraulic diameter of the microchannel. For the Tris-borate buffer solution in a microchannel of 120 μm in the hydraulic diameter, we can estimate the electroosmotic flow response time of order $\tau_{eof}=O\left(10^{-2}\right)$s. In experiment, the applied AC frequency is 10 kHz. The time period $\tau_{AC}\sim O(10^{-4})$ was two orders smaller than τ_{eof}. Hence, we can assume that the bulk flow is not able to response to the AC and the flow is only driven by the DC, i.e. $\vec{u}_{eof}=\mu_{eof}\vec{E}_{DC}$. The slip velocity then can be modified as

$$\vec{U}_s=-\frac{\varepsilon_m\varepsilon_0\zeta_w\vec{E}_{DC}}{\eta} \tag{6}$$

2.3 Solution and channel wall temperature fields

The Joule heating induced temperature field is governed by the energy equation expressed as

$$\rho c_p\vec{u}\cdot\nabla T=k_l\nabla^2T+\lambda(T)\vec{E}\cdot\vec{E} \tag{7}$$

where c_p and k_l are the specific heat and thermal conductivity of the buffer solution, respectively, and they are assumed to be constant. The combined electric field is expressed as $\vec{E}=\vec{E}_{AC}+\vec{E}_{DC}=\vec{A}\sin 2\pi ft+\vec{B}$, where *f* is the frequency of AC, $\left|\vec{A}\right|$ and $\left|\vec{B}\right|$ are the magnitude of AC and DC, respectively. Then the local time average Joule heat in a period can be expressed as

$$\overline{\lambda\vec{E}\cdot\vec{E}}=\frac{\lambda}{1/f}\int_0^{1/f}\vec{E}\cdot\vec{E}dt=\lambda\left|\frac{\vec{A}}{\sqrt{2}}\right|^2+\lambda\left|\vec{B}\right|^2=\lambda\vec{E}_{AC,\,rms}^2+\lambda\vec{E}_{DC}^2$$

which can be divided into two sections contributed by AC and DC, respectively. Here, $\vec{E}_{AC,\,rms}$ is the root mean square value of AC electric field strength. Thus, Eq. (7) averaged in a period can be modified as

$$\rho c_p\vec{u}\cdot\nabla T=k_l\nabla^2T+\lambda(T)\vec{E}_{AC,\,rms}^2+\lambda(T)\vec{E}_{DC}^2 \tag{8}$$

Hence, to generate the same amount of Joule heat compared with a sole DC, the DC component in the combined electric field can be greatly reduced when a high amplitude AC is combined together.

The buffer solution is continuously supplied from the inlet reservoir at room temperature, i.e. $T_{x=L}=T_0$, and is considered as thermally fully-developed at the outlet reservoir, i.e. $\left.\frac{\partial T}{\partial x}\right|_{x=0}=0$. Since the thermal boundary condition at the channel wall is unknown, a conjugate heat transfer problem has to be solved by simultaneously considering the heat conduction through the solid channel wall,

$$\rho_s c_{ps}\frac{\partial T}{\partial t}=k_s\nabla^2T \tag{9}$$

where ρ_s, c_{ps}, k_s are the specific heat , density, and thermal conductivity of the microchannel wall, respectively. The condition of natural convection heat transfer with room air is applied to the outside surfaces of the fabricated devices when solving the temperature field of the channel substrate. The heat transfer coefficient of natural convection is chosen to be 15 $Wm^{-2}K^{-1}$.

2.4 Sample solute concentration field

It is assumed that no adsorption of sample solutes onto the microchannel wall and no interaction between the sample solutes and the electrolyte components. Therefore, the sample solute concentration can be governed by the mass transport equation of the charged solutes

$$\frac{\partial C}{\partial t}+\nabla\cdot\left(\vec{u}C+\vec{u}_{ep}C\right)=\nabla\cdot\left[D(T)\nabla C\right] \tag{10}$$

where C is the concentration of sample solutes, and $D(T)$ is the mass diffusion coefficient of solutes, given by $D(T)=D_0\left[1+0.02\left(T-T_0\right)\right]$ [30]. D_0 is the mass diffusion coefficient of the solutes at room temperature T_0.

The time average electrophoretic velocity of the solutes $\vec{u}_{ep}$ can be simply expressed as $\vec{u}_{ep}=\mu_{ep}\vec{E}_{DC}$, where μ_{ep} is the temperature-dependent electrophoretic mobility of the sample solutes, given by [27]

$$\mu_{ep}=-4.394\times10^{-14}\times(T-273)^2-8.024\times10^{-10}\times(T-273)+8.621\times10^{-9}$$

At the initial time, the microchannel is filled with sample solution of the same concentration as those in the two

reservoirs, i.e. $C = C_0$. At the two reservoirs, $C_{x=0} = C_{x=L} = C_0$. And no mass transport is allowed to penetrate the channel wall surfaces.

2.5 Numerical method

COMSOL Multiphysics is utilized to numerically solve the above-described governing equations so as to obtain the electric field, velocity field, temperature field and concentration field. Since the channel geometry is symmetric, only half of the channel and glass slide is computed. A grid size independent test was conducted to ensure sufficient accuracy of numerical results. [29]

3. EXPERIMENT

3.1. Design and fabrication of microchannels

Fig. 1 shows a schematic diagram of the design and dimensions of the Poly-dimethylsiloxane (PDMS) channel. The entire microchannel has 10 mm in length and a uniform depth of 50 μm. Both the narrow channel region and the wide channel region have the same length of 5 mm. The widths of the narrow and wide channel regions are 120 μm, and 600 μm, respectively. SU8-50 was used to make the microchannel molds on a Si wafer by the photolithography technique. The PDMS microchannel was fabricated subsequently by using the soft-lithography technique. The process was detailed in previous report [29].

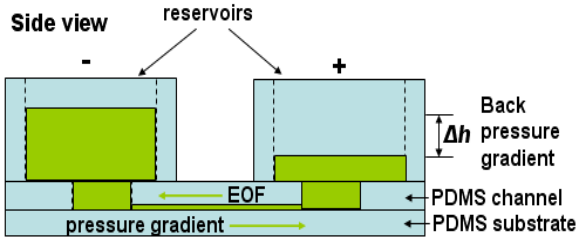

(a)

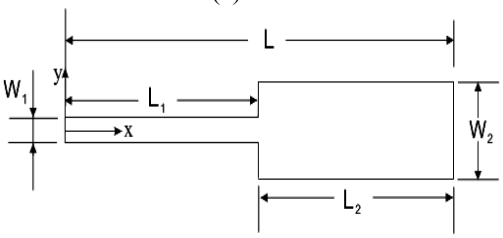

(b)

Fig.1 Schematic design of (a) a microfluidic device and (b) the PDMS channel dimensions

3.2. Preparation of buffer solution and sample solutes

Tris-borate buffer (Sigma-Aldrich) was used as buffer solution. Fluorescein-Na (Sigma-Aldrich) was used as sample solute for sample focusing experiment. Fluorescein-Na dye was initially dissolved in DI water at a concentration of 0.01mM and stored at -30℃ in a refrigerator. Prior to the focusing experiment the dye was further diluted to the required concentrations (0.5 μM or 0.05 μM) in 180 mM Tris-Borate buffer solutions. All solutions were filtered with a 0.2 μm syringe filter (Whatman, USA).

3.3. Experimental setup

The microchannel and two reservoirs were flushed with DI water and then filled with a sample solution. Two platinum wire electrodes with 0.5 mm in diameter (Sigma-Aldrich) were placed in each reservoir to generate the combined AC and DC electric fields by a function generator (Agilent 33250A) connected with a customized high voltage amplifier (Optrobio Technologies, Singapore). The generated signal can be monitored by an oscilloscope (CombiScope® HM 1008) to ensure the reliability of the applied AC voltage plus DC bias over the experiment.

Experiments were performed with a fluorescence microscope (Carl Zeiss, Germany) equipped with a 5x objective lens, a mercury arc lamp (mbq 52 ac, Zeiss) for fluorescent excitation, an appropriate filter set (excitation, 494nm; emission, 521nm) and a CCD camera (Sensovation AG, Germany) for acquiring optical fluorescence images.

3.4. Calibration

The relationship between the intensity of fluorescent signals and the intensity of grayscale images was calibrated the same as in previous study [29]. In our late focusing experiments, the fluorescent intensity values of processed images were converted into the corresponding concentrations using the calibration curve that is mathematically expressed by

$$C = A_0 + A_1 I + A_2 I^2 + A_3 I^3 \qquad (11)$$

where C and I are the fluorescein concentration and intensity, respectively, and $A_0 = 1.5084\,\mu\text{M}$, $A_1 = 1.0275\,\mu\text{M}$, $A_2 = -0.0027\,\mu\text{M}$ and $A_3 = 9E^{-6}\,\mu\text{M}$.

4. RESULTS AND DISCUSSION

4.1. Effect of the combined AC electric field component in the TGF

In experiment, the combined AC and DC electric field was applied to the microchannel instead of a sole DC electric field. Because the frequency of the applied AC electric field (10 kHz) is much higher than the frequency response of the fluid in the microchannel, the AC electric field can used to suppress the EOF and meanwhile contribute to produce the temperature gradient as previous analyzed. Due to the limitation of equipment, the maximum amplitude of AC electric field that the amplifier can supply is 400 V.

Fig. 2 shows the microscope images of TGF in the PDMS/PDMS microdevice under a sole DC electric field or the combined AC and DC electric field. The solution contains 0.5 μM Fluorescein-Na solute dissolved in the Tris-borate buffer. Initially, the microchannel was filled with the dilute Fluorescein-Na solution which was uniformly distributed within the channel. When a sole DC 450 V was applied, no focusing phenomena were observed (Fig. 2b). However, when the 400sinωt V AC combined with the DC 450 V was applied, the analytes were gradually focused near the conjunction section and the analyte concentration was observed to increase

with time (Fig. 2c). Similar concentration enhancement was observed when the sole DC voltage was increased to 600 V (Fig. 2d). The results demonstrated that the additional AC electric field can reduce the DC voltage required to obtain the similar concentration enhancement. The result also reflects the importance of temperature gradient in this concentration technique. The combined AC electric field contributed to produce the required temperature gradient for TGF, while the temperature gradient generated under the sole DC 450 V was not big enough to satisfy the focusing condition. The Joule heat generated by the combined AC and DC is comparable to the Joule heat generated by the sole DC, which can be estimated by

$$\left(\lambda\vec{E}^2_{AC,AC+DC}+\lambda\vec{E}^2_{DC,AC+DC}\right):\lambda\vec{E}^2_{DC,pureDC}=\left[\left(200\sqrt{2}\right)^2+450^2\right]:600^2=113:144$$

Fig. 3 shows that the concentration enhancement under 600 V DC is comparable but slightly higher than that under the combined AC and DC electric field. Furthermore, in experiment, it was found that when AC frequency was higher than 1 kHz, the AC frequency did not affect the sample concentration. When the applied AC frequency was lower than frequency response of the fluid, oscillation of EOF caused the focusing band shacking.

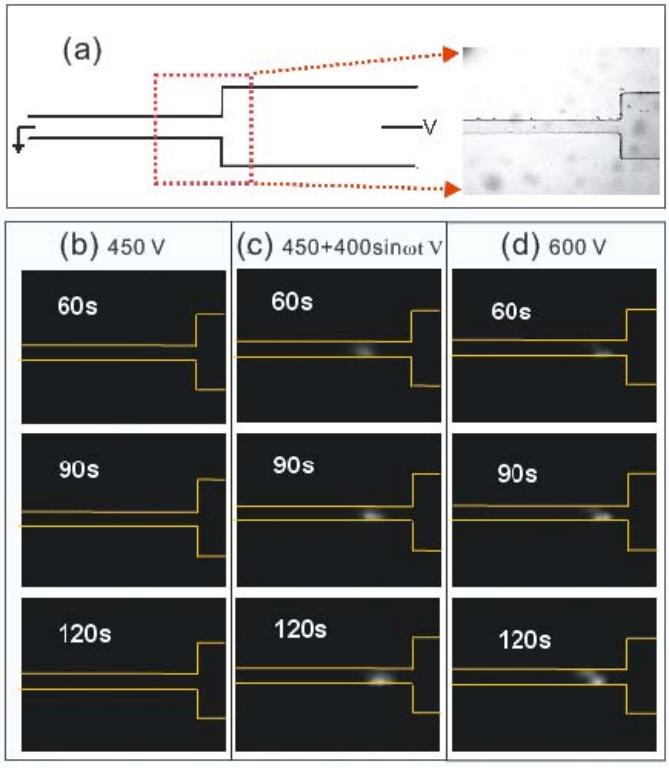

Fig.2 TGF using Joule heating induced temperature gradient under various applied voltages. (a) Microscopy image of the zoomed microchannel junction. Left reservoir is grounded, while the right reservoir is applied with a high voltage. (b-d) Microscopy fluorescence images taken at 60s, 90s, 120s, after the application of electrical voltages

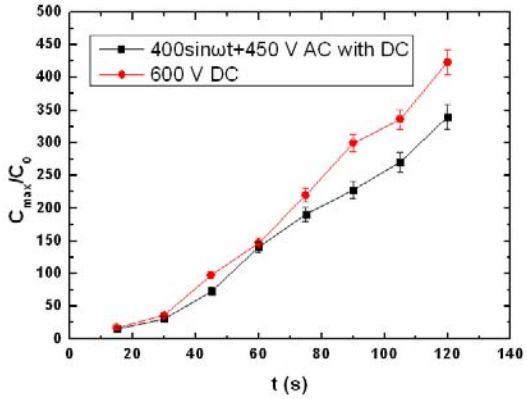

Fig.3 Concentration enhancements of TGF under a combined AC and DC electric field and a sole DC

4.2. Achiev ing high concentration factor under the combined AC and DC electric field

The net EOF driven by the DC electric field from the positive electrode side to the negative electrode side can cause a liquid level difference in the reservoirs which results in a backpressure gradient. The velocity component induced by the backpressure gradient can affect the analyte stagnant location, pushing the sample focusing zone moving to the positive electrode side. In order to reach higher concentration factors, the sample focusing zone should be maintained in the narrow channel region. To reduce the backpressure effect, a combined AC and DC electric field was recommended instead of a sole DC electric field. Moreover, two reservoirs with larger area (compared with the original reservoirs with a diameter of 6mm) were added to the microdevice to further reduce the backpressure effect due to the finite reservoir size (Fig. 1a).

In experiment, the solution contains an even dilute 0.05 μM Fluorescein-Na in the Tris-borate buffer. Fig. 4a shows the concentration enhancement achieved under the combined 400sinωt V AC with 450 V DC voltages with the reservoir area of 8mm × 12 mm. A more than 1200-fold concentration enhancement was achieved within 6 min. After 6 min, the focusing zone was moving close to the conjunction section, and the concentrated sample band was dispersed due to the sudden increasing of the channel area. Hence, the sample concentration decreased when the concentrated sample band was pushed across the conjunction by the backpressure effect. In order to achieve an even higher concentration factor, we further enlarged the reservoir area to 16 mm × 16 mm to increase the duration of sample concentration in the narrow channel region. As showed in Fig. 4b, a more than 2500-fold concentration enhancement was achieved within 14 minutes, which is the highest concentration factor demonstrated in TGF using inherent Joule heating effect, compared to the 300-fold concentration enhancement within 190s achieved by Ross and Locascio [18] and 200-fold concentration enhancement within 120s achieved by Kim et al. [26]. The concentrating speed here (2500-fold in 14 min) was also faster than the concentrating speed of TGF using external heating/cooling equipment (10000-fold in 100 min by Ross and Locascio [18]), and was

equivalent to the concentration performances using IEF (1000-fold in 5 min by Montgomery et al. [13]) and EFGF (4000-fold in 60 min by Liu et al. [15]). And the total length of microchannel here (1 cm) was much shorter than those used in IEF and EFGF (~5 cm), making it suitable for development of compact Lab-on-a-chip systems. Moreover, the operation of TGF using the combined AC and DC electric field is quite straightforward, with simple adjustment of AC or DC electric field strength to realize the concentration at desired location. And the microchannel is simple for design and easy for fabrication.

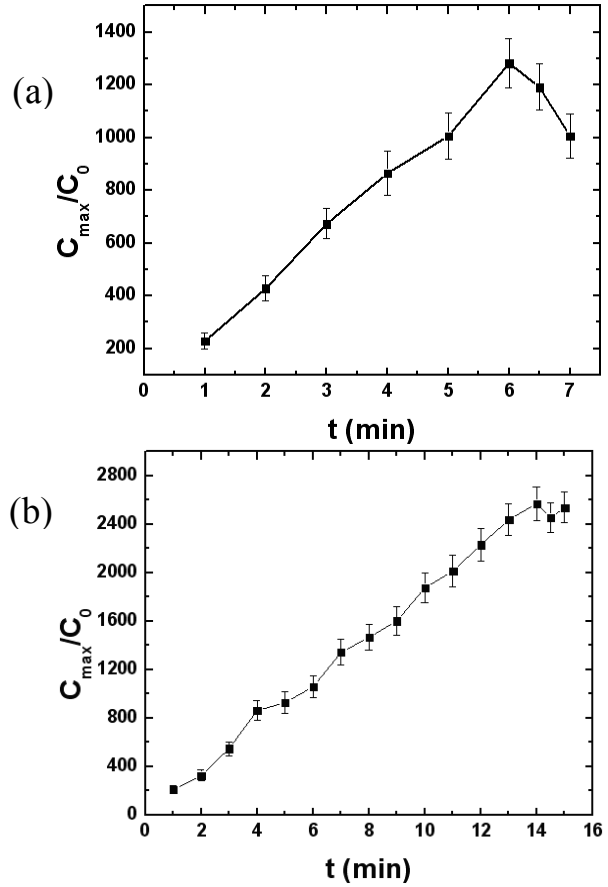

Fig.4 Concentration enhancements under the combined AC and DC electric fields with (a) the reservoir area of 8 mm × 12 mm (b) the reservoir area of 16 mm × 16 mm

Fig. 5 shows a comparison between the numerical simulations and the experimental results of the concentration enhancement for 0.05 μM fluorescein-Na during a focusing time of 14 min under the combined AC and DC electric field. The numerical simulation reasonable agrees with the experimental data, through the prediction is higher than the experimental result. Because the phenomena are complicated, lots of factors can affect the TGF results. In the model assumptions, the reservoir and backpressure effects are neglected. The interaction between sample solutes and buffer solution is not considered, as well as the dispersion effect. The absorption of solutes and swelling of PMDS can also contributed to the discrepancy between our numerical model predictions and experimental data. More importantly, photobleaching of the fluorescent solutes is a significant factor that can lead to the underestimated the concentration enhancement in the experimental results.

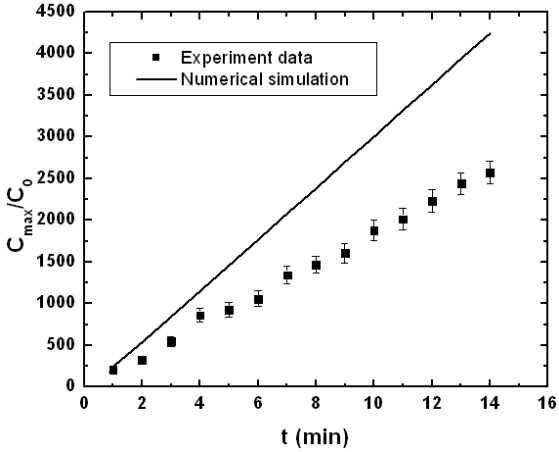

Fig.5 Comparison between experimental data and numerical results of the normalized concentration versus time

Photobleaching is a destructive process where the fluorophore loses the ability to emit light under prolonged exposure to excitation. The rate of photobleaching depends on a number of factors including illumination intensity and wavelength, exposure time and so on. According to Gui and Ren [31], when fluorescent dyes of a concentration C_0 were exposed under an excitation light intensity I, the remaining dye concentration C after an exposure time t can be expressed as

$$C / C_0 = e^{-kIt} \tag{12}$$

where k is a coefficient considering of the dye photobleaching speed. Experiments were carried out to find this coefficient. Standard 200 μM fluorescein dye solution was filled in the channel and exposed under the same illumination intensity as in the TGF experiments. The captured intensities were converted into the corresponding dye concentrations using Eq. (11) and the relationship was mathematically expressed as $C / C_0 = e^{-0.042t}$, as shown in Fig. 6. There were 92% fluorescein dyes remaining in the solution after 2 min, while only 56% dyes remaining after 14min. This indicates that concentration (2500-fold) of sample solutes converted from image intensity, which is only the concentration of the remaining solute dyes, is greatly underestimated compared to the actually concentration of solute dyes after 14 min.

5. CONCLUSIONS

This paper reports effects of the combined AC and DC electric fields in TGF with Joule heating in a microchannel with a sudden expansion in the cross-section. A theoretical model including a set of governing equations is developed for the TGF under the combined electric fields. Experimental results show that the high frequency AC electric field which contributes to produce the temperature gradient can reduce the

required DC voltage to achieve the sample concentration. The smaller DC voltage will result in a smaller EOF, which can reduce the backpressure effect due to the finite reservoir sizes. Backpressure effect was observed experimentally which made the concentrated sample zone moving to the positive electrode side. Additionally, two reservoirs with larger area are added to the microdevice to further reduce the backpressure effect and accordingly increase the duration of sample focusing in the narrow channel region. A more than 2500-fold concentration enhancement was obtained within 14 min in our PDMS/PDMS microdevice, which is a great achievement in TGF using inherent Joule heating effect. Numerical simulation shows a higher prediction than the experimental results. Photobleaching was investigated experimentally, which indicated an underestimated of concentration enhancement of experimental results. Further studies are needed to quantify the photobleaching effect in our TGF processes.

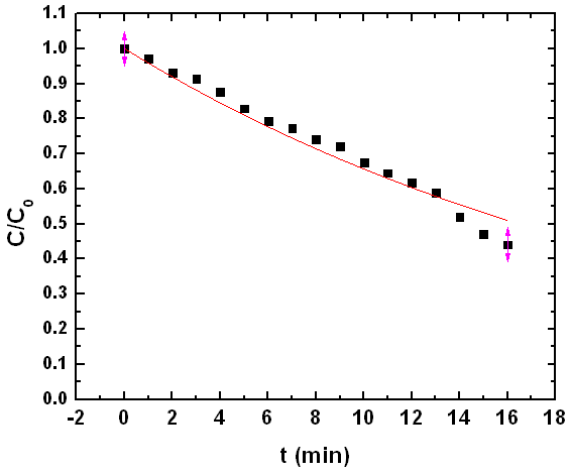

Fig.6 Photobleaching of fluorescein dyes in TGF experiment

ACKNOWLEDGMENTS

The authors gratefully acknowledge the financial support of the research grant (MOE2009-T2-2-102) from the Ministry of Education of Singapore to CY and the Ph.D. scholarship from Nanyang Technological University to ZWG.

REFERENCES

[1] Psaltis, D.; Quake, S. R.; Yang, C., Nature 2006, 442, 27, 381-386.
[2] Yager, P.; Edwards, T.; Fu, E.; Helton, K.; Nelson, K.; Tam, M.R.; Weigl, B.H.; Nature 2006, 442, 27, 412-418.
[3] Whitesides, G. M.; Nature 2006, 442, 368-373.
[4] Dittrich, P. S.; Tachikawa, K.; Manz, A.; Anal. Chem. 2006, 78, 3887-3908.
[5] Burgi, D. S.; Chien, R. L.; Anal. Chem. 1991, 63, 2042-2047.
[6] Zhang, C. X.; Thormann, W.; Anal. Chem. 1996, 68, 2523-2532.
[7] Beckers, J. L.; Bocek, P.; Electrophoresis 2000, 21, 2747-67.
[8] Quirino, J. P.; Terabe, S.; Science 1998, 282, 465-468.
[9] Ma, B., Zhou, X.M., Wang, G., and Huang, H.Q., Electrophoresis 2006, 27, 4904-4909
[10] Jung, B., Bharadwaj, R., and Santiago, J.G., Analytical Chemistry 2006, 78, 2319-2327
[11] Malá, Z.; Ludmila, K.; Gebauer, P.; Bocek, P.; Electrophoresis 2007, 28, 243-253.
[12] Shim, J.; Dutta, P.; Ivory, C. F.; Electrophoresis 2008, 29, 1026-1035.
[13] Montgomery, R.; Jia, X. G.; Tolley, L.; Anal. Chem. 2006, 78, 6511-6518.
[14] Mosher, R. A.; Thormann, W.; Electrohoresis 2008, 29, 1036-1047.
[15] Liu, J.; Sun, X.; Farnsworth, P. B.; Lee, M. L.; Anal. Chem. 2006, 78, 4654.
[16] Petsev, D. N.; Lopez, G. P.; Ivory, C. F.; Sibbett, S. S.; Lab Chip 2005, 5, 587–597.
[17] Humble, P. H.; Kelly, R. T.; Woolley, A. T.; Tolley, H. D.; Lee, M. L.; Anal. Chem. 2004, 76, 5641-5648.
[18] Ross, D.; Locascio, L.E.; Anal. Chem. 2002, 74, 2556-2564.
[19] Balss, K. M.; Vreeland, W. N.; Howell, P. B.; Henry, A. C.; Ross, D.; J. AM. CHEM. SOC. 2004, 126, 1936-1937.
[20] Munson, M. S.; Danger, G.; Shackman, J. G.; Ross, D.; Anal. Chem. 2007, 79, 6201-6207.
[21] Balss, K.M.; Ross, D.; Begley, H. C.; Olsen, K.G.; Tarlov, M.J.; J. AM. CHEM. SOC. 2004, 126, 13474-13479.
[22] Balss, K. M.; Vreeland, W. N.; Phinney, K. W.; Ross, D.; Anal. Chem. 2004, 76, 7243-7249.
[23] Lin, H.; Shackman, J.G.; Ross, D.; Lab Chip 2008, 8, 969-978.
[24] Huber, D.; Santiago, J.G.; J. Heat Transfer-Transactions ASME 2005, 127, 806-806.
[25] Huber, D.; Santiago, J.G.; Electrophoresis 2007, 28, 2333-2344.
[26] Kim, S. M.; Sommer, G. J.; Burns, M. A.; Hasselbrink, E. F.; Anal. Chem. 2006, 78, 8028-8035.
[27] Sommer, G. J.; Kim, S. M.; Littrell, R. J.; Hasselbrink, E. F.; Lab Chip 2007, 7, 898-907.
[28] Tang, G. Y.; Yang, C.; Electrophoresis 2008, 29, 1006-1012.
[29] Ge, Z.; Yang, C.; Int. J. Heat Mass Transfer 2010, 53, 2722-2731.
[30] Weast, R.; Astle, M. J.; Beyer, W. H.; CRC handbook of Chemistry and Physics, CRC Press Inc., Boca Raton, FL 1986.
[31] Gui, L.; Ren, C. L.; Applied Physics Letters 2008, 92, 024102